Colloids and Surfaces B: Biointerfaces 155 (2017) 200–208

Contents lists available at ScienceDirect

Colloids and Surfaces B: Biointerfaces

journal homepage: www.elsevier.com/locate/colsurfb

Stealth recombinant human serum albumin nanoparticles conjugating 5-fluorouracil augmented drug delivery and cytotoxicity in human colon cancer, HT-29 cells

Ankita Sharma [a], Amanpreet Kaur [a], Upendra Kumar Jain [a], Ramesh Chandra [b,c], Jitender Madan [a,*]

[a] Department of Pharmaceutics, Chandigarh College of Pharmacy, Mohali, Panjab, India
[b] Dr. B.R Ambedkar Centre for Biomedical Research, University of Delhi, Delhi, India
[c] Department of Chemistry, University of Delhi, Delhi, India

ARTICLE INFO

Article history:
Received 23 November 2016
Received in revised form 6 April 2017
Accepted 10 April 2017
Available online 12 April 2017

Keywords:
5-Fluorouracil
Recombinant human serum albumin
Poly (ethylene glycol)
Conjugation
Cytotoxicity
Pharmacokinetic

ABSTRACT

Background and objective: 5-Fluorouracil (5-FU) is a first-line chemotherapeutic drug in colorectal cancer. However, intravenous administration of 5-FU at the dose of 7–12 mg/kg exhibits curbs like short half-life (20 min) and toxic side-effects on bone marrow cells. Therefore, in present investigation, 5-FU was conjugated to poly (ethylene glycol) anchored recombinant human serum albumin nanoparticles (5-FU-rHSA-PEG-NPs) to improve the pharmacokinetic and therapeutic profiles.

Methods and results: The mean particle size of 5-FU-rHSA-NPs was measured to be 44.3 ± 5.8-nm, significantly ($P < 0.05$) lesser than 65.7 ± 7.2-nm of 5-FU-rHSA-PEG-NPs. In addition, zeta-potential of 5-FU-rHSA-NPs was estimated to be −10.2 ± 2.6-mV significantly ($P < 0.05$) lower than −25.8 ± 3.5-mV of 5-FU-rHSA-PEG-NPs. Moreover, both 5-FU-rHSA-NPs and 5-FU-rHSA-PEG-NPs were smooth, spherical and regular in shape. *In-vitro* drug release analysis indicated that 5-FU-rHSA-NPs and 5-FU-rHSA-PEG-NPs separately released 10.9% and 9.23% of 5-FU in PBS (pH ~ 7.4) with no significant difference ($P > 0.05$) up to 48 h. However, addition of 20% v/v serum to PBS (pH ~ 7.4) boosted the drug release. 5-FU-rHSA-NPs and 5-FU-rHSA-PEG-NPs released 78.26% and 48.9% of the 5-FU up to 48 h in presence of PBS (pH ~ 7.4 and 20% serum) with significant difference ($P < 0.05$). Furthermore, 5-FU-rHSA-PEG-NPs displayed the IC_{50} of 3.7-μM significantly ($P < 0.05$) lower than 6.8-μM and 11.2-μM of 5-FU-rHSA-NPs and 5-FU solution, respectively. One compartmental pharmacokinetic elements indicated that 5-FU-rHSA-PEG-NPs demonstrated the half-life ($t_{1/2}$) of 5.33 ± 0.15-h significantly ($P < 0.001$) higher than 1.50 ± 0.08-h and 0.30 ± 0.09-h of 5-FU-rHSA-NPs and 5-FU solution, respectively.

Conclusion: 5-FU-rHSA-PEG-NPs tendered improved cytotoxicity and pharmacokinetic profile. Hence, 5-FU-rHSA-PEG-NPs must be further tested under stringent *milieu* for translating in to a clinical product.

1. Introduction

Despite noteworthy advances in cancer chemotherapy, currently used chemotherapeutic agents are unable to recover the prognosis of advanced or recurrent colorectal cancer. The transport of existing chemotherapeutic drugs by particulate or colloidal nanocomposite has displayed lucrative advantages in terms of improved penetration in tumour tissues, high bioavailability at the site of action, augmented therapeutic index and reduced toxicity to normal tissues [1]. United-States Food and Drug Administration (US-FDA) has approved various anticancer drugs including 5-fluorouracil (5-FU), bevacizumab, avastin, capecitabine, oxaliplatin and irinotecan for the treatment of colon cancer [2,3]. However, 5-FU is used as a first-line chemotherapeutic drug in colorectal cancer, and instantly after surgery, is used as an adjuvant therapy. Chemically, 5-FU (5-Fluoro-2,4-pyrimidinedione) is an antimetabolite pyrimidine analogue that exhibits potent anticancer activity against broad spectrum of solid tumours like pancreas, liver, and colon [4–6]. Mechanistically, 5-FU hinders the action of enzyme thymidylate synthase and consequently prohibits the synthesis of pyrimidine thymidine, a nucleoside requisite for DNA replication [7]. It has been reported that 5-FU metabolite, fluorouridine triphosphate (FUTP) disrupts the RNA processing and functions in both human colon as well as breast cancer cells [8].

* Corresponding author.
E-mail address: jitenderpharmacy@gmail.com (J. Madan).

http://dx.doi.org/10.1016/j.colsurfb.2017.04.020
0927-7765/

Owing to erratic absorption and hampered bioavailability, 5-FU is administered as intravenous (*i.v*) infusion at the dose of 7–12 mg/kg for 4 days for successive chemotherapy [9]. However, 5-FU has certain curtails like short biological half-life (20 min) due to rapid metabolism [10] and toxic side-effects on bone marrow cells [11]. Therefore, several attempts were undertaken to improve the delivery of 5-FU from both oral and parenteral route of administration. Liposomes, microspheres, and polymeric nanoparticles have been reported to perk up the therapeutic efficacy of 5-FU [12–15]. Nevertheless, therapeutic efficacy of encapsulated 5-FU in nano/micro carriers was impinged owing to superfluous release that consequently delivered subtherapeutic pay load in vicinity of the tumour cells. In addition, only few attempts have been embarked previously including 5-FU-lipid drug conjugate, 5-FU conjugated gold nanoparticles, 5-FU-dendrimer conjugate, and dual drug conjugate (imatinib and 5-FU) for improving the anticancer potential of 5-FU in cancer cells [16–19].

Human serum albumin (HSA) with an average half-life of 19 days, is a biocompatible, biodegradable and non-immunogenic biopolymer [20,21]. Recombinant human serum albumin (rHSA) offers lucrative merits like avoidance of potential risk of contamination by blood-derived pathogens and profuse supply [22]. Moreover, rHSA is amphiphilic in nature owing to surfactant traits that prevents protein aggregation, stabilizes the conformational structure of therapeutic moiety and maintains its bioactivity throughout the shelf-life of product [23]. Besides, rHSA is also used as a cryoprotectant owing to high glass transition temperature [24]. Recently, US-FDA has approved paclitaxel-rHSA conjugate (Abraxane®) for site-specific delivery. This product offered improved tumour targeting due to enhanced permeation and retention (EPR) effect as compared to free drug [25].

Several chemotherapeutic drugs have been encapsulated in HSA nano/micro carriers for targeting tumour tissues through parenteral routes of administration [26–28]. Furthermore, albumin based nanocarriers accumulate more frequently in tumour tissues owing to EPR attribute [29,30]. The augmented EPR effect of albumin based nanocarriers may be ascribed to the fact that solid tumours commonly enjoy an immature, highly porous vasculature that is acted upon by vascular permeability enhancing factors like nitric oxide. However, tumour vasculature lacks adequate lymphatic drainage. As a consequence, macromolecules (>40 kDa) accumulate within the tumour interstitium due to EPR effect. Tumour is also a site for albumin catabolism. Tumours consume albumin as a source of energy, split albumin into amino acids in lysosomes that are subsequently exercised by cancer cells for accelerating their growth and progression [31]. This was also supported by hypoalbuminiemia in cancer patients as a result of albumin catabolism in tumour tissues [32].

PEGylation of nanoscaled drug delivery systems offered superior circulation half-life [33] and abridged toxicity of protein. Polyethylene glycol (PEG) is advantageous owing to its low toxicity, squat immunogenicity and high biocompatibility [34–36]. PEG has capability to protect the protein against enzymatic degradation and engulfment by reticuloendothelial system (RES) [37,38]. The density of PEG overlays a stearic barrier on to the surface of nanoparticles by means of its hydrophilic chains and thereby reduces the opportunity of opsonization and phagocytosis of nanoparticles. Therefore, in present investigation, initially 5-FU was conjugated to rHSA and later, 5-FU-rHSA was chemically coupled to poly (ethylene glycol) monoamine (5-FU-rHSA-PEG) for tailoring hydrophilic layer. Next, 5-FU-rHSA-PEG nanoparticles (5-FU-rHSA-PEG-NPs) and unmodified nanoparticles (5-FU-rHSA-NPs) were formulated by desolvation technique [39] and characterized *in vitro* using various analytical, spectral and biological techniques. The pharmacokinetic profile of 5-FU-rHSA-PEG-NPs, 5-FU-rHSA-NPs and 5-FU solution was analyzed in Swiss albino male mice following *i.v* route of administration *as per* the recommended dose-dosage regimen.

2. Materials and methods

2.1. Chemicals

5-FU ($M_w \sim 130.077$) was obtained as a gift sample from Arbro Pharmaceuticals, New Delhi, India. Recombinant human serum albumin (rHSA; α-lysine amino acids ~62, $M_w \sim 66.5$ kDa, Purity ~ 96–99%) was purchased from Himedia, Mumbai, India. Poly (ethylene glycol) monoamine ($M_w \sim 5000$) was obtained from Sigma-Aldrich, USA. *N*-(3-dimethylaminopropyl)-*N*-ethylcarbodiimide hydrochloride (EDAC.HCl) and *N*-hydroxy succinimide (NHS) were purchased from Molychem, Mumbai, India. All other chemicals used were of highest analytical grade.

2.2. Cell culture and mediums

Human colon cancer cell line (HT-29) was maintained in 95% air and 5% CO_2 at 37 °C using Dulbecco's Modified Eagle's Medium (DMEM) (Biologicals, Israel) supplemented with 10% fetal bovine serum. All experiments were performed with asynchronous population in exponential growth phase (24 h after plating) [40].

2.3. Synthesis of 5-fluorouracil coupled poly (ethylene) glycol conjugated recombinant human serum albumin

2.3.1. Synthesis of 5-fluorouracil acetate

The synthesis of 5-fluorouracil acetate was instigated with alkylation that leads to the formation of an intermediate product, 5-flurouracil-methyl ester (Scheme 1) [41]. In brief, 5-FU (0.005 M, 0.65 gm) was dissolved in α-chloroacetic acid methyl ester (0.01 M, 1.8 gm) in addition to 100 mg of freshly prepared potassium carbonate. Subsequently, 40 ml of dimethyl formamide was added to the reaction mixture followed by stirring at room temperature for 14–18 h. The completion of the reaction was verified by thin layer chromatography (TLC) using 20% ethyl acetate: hexane mixture as mobile phase. Finally, the mixture was poured into the crushed ice and precipitates of 5-FU-CH_2COOCH_3 were filtered off, and dried. The yield of 5-FU-CH_2COOCH_3 was estimated to be 78.4%. The synthesis of 5-FU-CH_2-$COOCH_3$ was confirmed by ^{1}H NMR spectroscopy using BRUKER DPX 300 MHz spectrophotometer. The ^{1}H NMR of 5-FU was also captured for comparison.

Next, hydrolysis of 5-FU-CH_2COOCH_3 was carried out to yield 5-FU-CH_2COOH (Scheme 1) [42]. In an experiment, 1.0 g of 5-FU-CH_2COOCH_3 was mixed with 10 ml of 10% NaOH solution and the reaction mixture was stirred for 2–12 h at room temperature. The completion of the reaction was verified by TLC using 20% ethyl acetate: hexane as mobile phase. Finally, the solution was neutralized with 4 N HCl and extracted with 50 ml of ethyl acetate and 50 ml of water. The end product was dried over sodium sulphate followed by distillation that eventually supplied 5-FU-CH_2COOH (Scheme 1). The yield of 5-FU-CH_2COOH was measured to be 67.8%. The synthesis of 5-FU-CH_2COOH was confirmed by ^{1}H NMR spectroscopy, as specified earlier.

2.3.2. Synthesis of 5-fluorourcil coupled recombinant human serum albumin

5-Fluorourcil coupled recombinant human serum albumin (5-FU-rHSA) was synthesised by covalent-coupling method (Scheme 1) [43]. Briefly, 5-FU-CH_2COOH (0.188 g, 0.1 M), EDAC.HCl (0.384 g, 0.2 M) and NHS (0.23 g, 0.2 M) were added to 100 ml of phosphate buffer of pH ~ 4.7. Following this, 0.665 g (100 μM) of rHSA was added to the buffer and stirred overnight. Next day, 5-FU-rHSA was purified by dialysis against distilled water for 8 h.

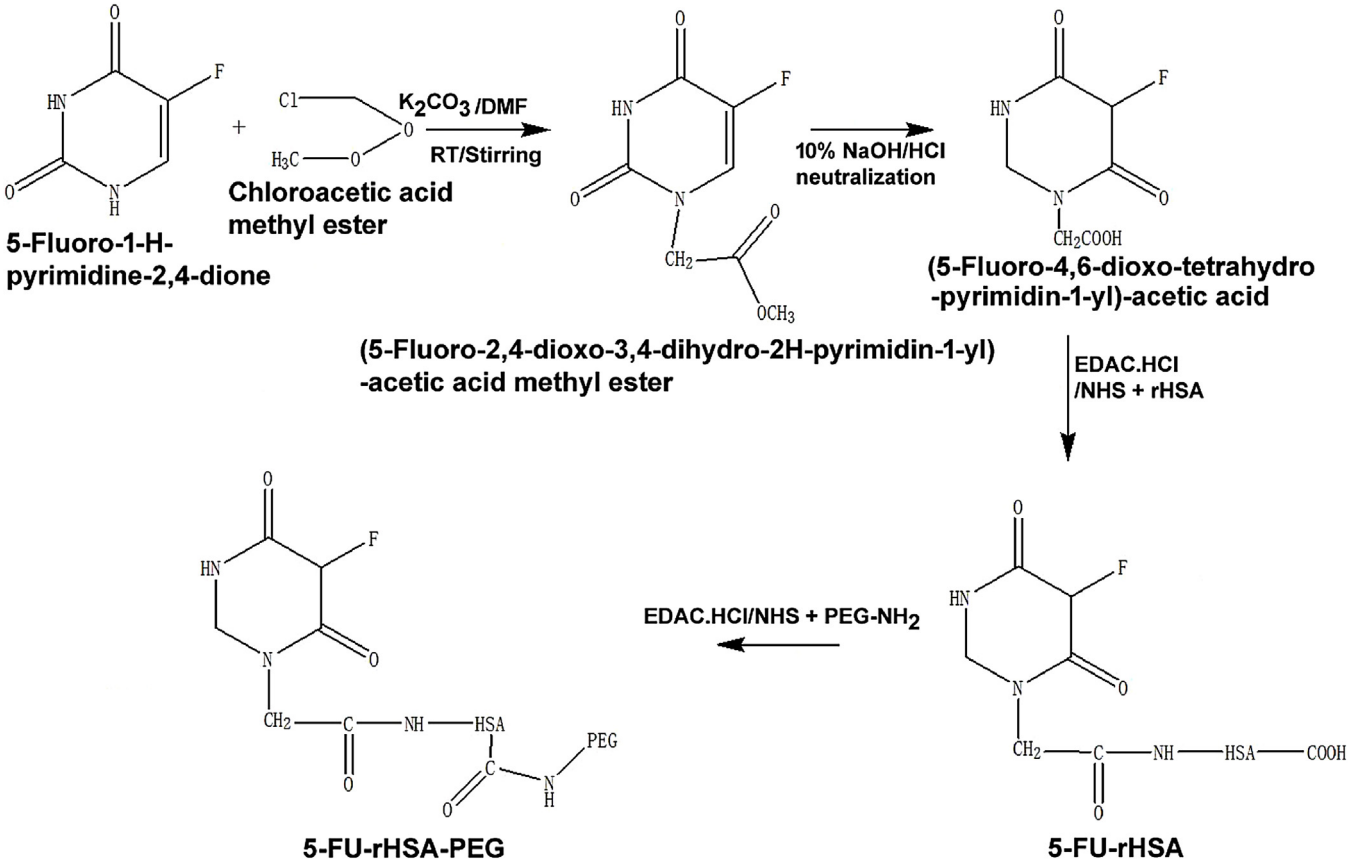

Scheme 1. Schematic representation of the steps involved in synthesis of 5-FU-rHSA-PEG.

The synthesis of 5-FU-rHSA was confirmed by FT-IR (Perkin Elmer, Massachussetts, USA) spectroscopy and compared with spectrum of 5-FU. Samples were prepared using KBr pellet (5 mg sample in 200 mg KBr) at a force of 40 psi for 5 min with a hydrostatic press. Spectra were recorded in the range of 4000–400 cm^{-1} at a resolution of 4 cm^{-1}.

2.3.3. Determination of conjugation efficiency of 5-fluorouracil to recombinant human serum albumin

Conjugation efficiency was analyzed by Bradford assay method [44]. For testing, 1 mg of rHSA or 5-FU-rHSA was added to 10 ml of distilled water. From this stock solution, 2 ml of the sample was withdrawn and added to a mixture of 1.5 ml of Bradford reagent and 1.5 ml of distilled water. All test tubes were incubated at room temperature for 10 min. Samples were filtered through 0.22-μm membrane filter (MDI, Ambala, India) and the absorbance of each filtrate was measured at 595 nm using a UV/Visible spectrophotometer (1800, Shimadzu, Kyoto, Japan). The conjugation efficiency was calculated from the following formula:

$$\%\ Conjugation\ efficiency = A\ of\ conjugated\ amines \frac{(A\ of\ amines\ in\ rHSA - A\ of\ amines\ in\ conjugated\ rHSA) \times 100}{A\ of\ amines\ in\ rHSA}$$

Where A = absorbance

2.3.4. Synthesis of poly (ethylene glycol) conjugated recombinant human serum albumin coupling 5-fluorouracil

5-FU-rHSA was conjugated to poly (ethylene glycol) monoamine (5-FU-rHSA-PEG) by covalent-coupling technique [43]. In brief, 0.2 g of 5-FU-rHSA was added to 20 ml of phosphate buffer (pH ~ 4.7) containing EDAC.HCl (0.152 g, 4 mM) and NHS (0.092 g, 4 mM). Following this, mixture was stirred at room temperature for 4 h. In last, poly (ethylene glycol) monoamine (2 mM, 0.2 g) was added to the solution and stirred for next 24 h to yield 5-FU-rHSA-PEG (Scheme 1). The synthesis of 5-FU-rHSA-PEG was confirmed by FT-IR spectroscopy, as specified earlier.

2.3.5. SDS-PAGE analysis

The SDS-PAGE assay was performed on 12% polyacrylamide gel to determine the molecular mass of 5-FU-rHSA and 5-FU-rHSA-PEG, respectively. In brief, rHSA, 5-FU-rHSA and 5-FU-rHSA-PEG in equal concentration (100 μg/ml) were separately diluted in 1 M Tris HCl buffer (pH ~ 6.8) containing 10% SDS, 11.6% (v/v) glycerol and 1% bromophenol blue with 1% β-mercaptoethanol. All samples were heated for 10 min in a boiling water bath and later loaded on to the gel to analyze the molecular mass.

2.4. Preparation of poly (ethylene glycol) conjugated recombinant human serum albumin nanoparticles coupling 5-fluorouracil

Poly (ethylene glycol) conjugated recombinant human serum albumin nanoparticles coupling 5-fluorouracil (5-FU-rHSA-PEG-NPs) were prepared by desolvation technique [39]. 50 mg of 5-FU-rHSA-PEG was dissolved in 25 ml of distilled water to form the aqueous phase. Subsequently, acetone (5 ml) [45] was added to the aqueous phase at the rate of 1 ml/min under constant stirring at room temperature. Following desolvation process, 25% v/v glutraldehyde solution (50 μl) was included in the mixture to crosslink the desolvated nanoparticles. Stirring was continued for next 24 h at room temperature for efficient cross-linking. Later, tailored

nanoparticles were purified by centrifugation (Sorvall Ultracentrifuge, Thermo Fisher Scientific, Waltham, Massachusetts, United States) at 30,000 rpm for 1 h and redispersed in distilled water. Finally, nanoparticles dispersion was freeze-dried (Lark Technology, Chennai, India) to get the fine powder. Correspondingly, 5-FU-rHSA-NPs were also formulated for comparative studies.

2.5. Characterization of nanoparticles

2.5.1. Particle size and zeta-potential

Particle size and zeta-potential of nanoparticles were determined by Malvern Nano ZS (Malvern Instruments, Worcestershire, UK). Each nanoparticle sample (5 mg) was separately suspended in 10 ml of phosphate buffer saline (PBS, pH ~ 7.4) and particle size was measured. An electric field of 150 mV was applied to determine the electrophoretic velocity of nanoparticles. All measurements were carried out in triplicate (n = 3).

2.5.2. Transmission electron microscopy

Transmission electron microscopy (TEM, FTI Tecnai F20) was used to visualize the nanoparticle shape. For this purpose, an aqueous dispersion of each nanoparticle sample was drop casted onto a carbon coated copper grid, and the grid was air dried at room temperature before loading it into the microscope which was maintained at a voltage of 80 kV.

2.5.3. Powder x-ray diffraction pattern

The lattice structure of nanoparticles was validated by X-ray diffractometer (X'Pert PRO, Panalytical Company, Almelo, The Netherlands) using Ni-filtered, Cu Kα-radiation, voltage of 60 Kv and a current of 50 mA. The scanning rate used was 1°/min over 5° to 80° diffraction angle at 2θ. The PXRD pattern of 5-FU, 5-FU-rHSA-NPs, and 5-FU-rHSA-PEG-NPs was recorded. The crystal size of 5-FU, 5-FU-rHSA-NPs and 5-FU-rHSA-PEG-NPs was measured using Scherer equation [46].

$Dp = \frac{0.94\lambda}{\frac{\beta}{2}} Cos\theta$ Where Dp refers to average crystallite size, β = Line broadening in radians, θ = Bragg angle λ = X-ray wavelength

2.5.4. In-vitro drug release

In vitro release of drug from tailored nanoformulations was measured using dialysis membrane technique [47]. Experimentally, 2 ml dispersion containing 12 mg of 5-FU or 472 mg of 5-FU-rHSA-PEG (~12 mg of 5-FU) or 439 mg of 5-FU-rHSA (~12 mg of 5-FU) was added to a dialysis bag (12 Kda pore size). The bags were then suspended separately in 900 ml of PBS (pH ~ 7.4) and PBS (pH ~ 7.4) containing 20% v/v fetal bovine serum that maintained at 37 °C and 100 rpm, as recommended for dissolution testing of parenteral products [48]. At 0.083, 0.25, 0.5, 1, 2, 4, 8, 16, 24, and 48 h, 5 ml of the sample was withdrawn and concurrently replaced with fresh dissolution medium to maintain the sink condition. The drug concentration was measured after filtration through 0.22 μm membrane filter (MDI, Ambala, India) at 265 nm [49] by using a UV/Visible spectrophotometer (1800, Shimadzu, Kyoto, Japan).

2.6. Comparative therapeutic efficacy testing of 5-FU-rHSA-PEG-NPs and 5-FU-rHSA-NPs

2.6.1. Standard cell proliferation assay

In vitro cytotoxicity was determined by MTT assay (3-[4,5-dimethylthiazol-2-yl]-2,5 diphenyltetrazolium bromide) [50]. Concisely, 7×10^3 HT-29 cells were plated in 200 μl of serum DMEM suspended in each well of a 96-wells microtitre plate (Tarsons, India). Post incubation period of 24 h, the serum DMEM was replaced with serum free-DMEM. Subsequently, HT-29 cells were exposed to a gradient concentration of 2–16 μM of 5-FU, 5-FU-rHSA-NPs, and 5-FU-rHSA-PEG-NPs for 72 h. In last, control and treated cells were incubated with MTT dye at a concentration of 5 mg/ml for 4 h at 37 °C. Subsequent to lysis of the cells, formazon crystals were obtained, which were solubilised in 100 μl of dimethyl sulfoxide. The absorbance was read at 570 nm using 630 nm as a reference wavelength by ELISA Reader (Tecan, Switzerland). The results were expressed as IC_{50}. The IC_{50} refers to the concentration of drug required to kill 50% of the cells.

2.6.2. Pharmacokinetic analysis

Pharmacokinetic analysis of 5-FU solution, 5-FU-rHSA-NPs, and 5-FU-rHSA-PEG-NPs was carried out using high-performance liquid chromatography (HPLC) by determining the concentration of 5-FU in plasma. HPLC system of Agilent Technologies 1220 infinity LC was used. The chromatographic separation was achieved in a reverse phase C18 column (4.6 mm × 150 mm) packed with particles of 5 μm. The mobile phase was consisted of acetonitrile: water (10: 90) mixture [51] that was filtered through 0.45-μm membrane filter (MDI, Ambala, India). The flow rate of mobile phase was adjusted at 1 ml/min. The samples were detected at a wavelength of 265 nm [49] and the detector was set at 0.005 absorbance unit, full scale.

The pharmacokinetic study was carried out according to guidelines of the Committee for the Purpose of Control and Supervision of Experiments on Animals (CPCSEA), Ministry of Culture, Government of India. Swiss albino male mice weighing 20–25 g were maintained on standard laboratory chow and water *ad libitum* in a temperature and light-controlled environment at Chandigarh College of Pharmacy, Mohali, Punjab, India. The Institutional Animal Ethics Committee (IAEC, Registration number: 1201/PO/Re/S/08/CPCSEA) had approved the study In short, 66 mice were randomly subdivided into 22 groups of three animals each. These 22 groups were further categorized as group A, B, and C. Though this gives us three mice *per* time point for analysis, but to make sure that our systemic error is acceptable, we had analyzed each sample in triplicate (n=3) and no variation was seen (at 95% confidence level). In group A, 5-FU infusion (12 mg/kg) [9] was administered *i.v.* through tail vein of the mice. Group B and C were administered 5-FU-rHSA-NPs (~12 mg/kg of 5-FU) and 5-FU-rHSA-PEG-NPs (~12 mg/kg of 5-FU) respectively through *i.v* route. The blood samples were collected from retro-orbital plexuses and stored in polypropylene microcentrifuge tubes containing 100 μl of sodium citrate (10% w/v), as an anticoagulant. Samples were centrifuged at 4600 rpm for 15 min (Remi, Mumbai, India) and plasma was collected. Plasma samples were stored at −20 °C until analyzed. Plasma concentration data were analyzed with standard one-compartmental method using WINNONLIN (Software version 4.1; Pharsight, California, USA) software. The pharmacokinetic parameters like k_e (elimination rate constant, h^{-1}), $t_{1/2}$ (half life, h), AUC_{last} (area under the curve up to last sampling point, h μg/ml), AUC_{inf} (area under the curve up to infinite, h μg/ml), AUMC (h^2 μg/ml), MRT (mean residence time, h), CL_{Total} (total clearance rate, l/h), and V_d (volume of distribution, l) were computed and compiled. The area under the curve (AUC_{last}) was calculated using the linear trapezoidal rule up to the last sampling point with detectable levels with extrapolation to infinity (AUC_{inf}) by Eq. (1):

$$AUCinf = AUClast + C/ke \quad (1)$$

k_e represents the elimination rate constant and it was calculated from the slope of the data points in final log linear part of the drug-concentration-time curve by least square linear regression analysis. The terminal disposition half-life ($t_{1/2}$) was calculated using Eq. (2):

$$t\frac{1}{2} = 0.693/ke \quad (2)$$

MRT (mean residence time) was calculated from the AUC_{last} and AUMC as seen in Eq. (3): AUMC was obtained from a plot of product of plasma drug concentration and time (C.t.) vis-à-vis '*t*' from zero to infinity.

$$MRT = AUMC/AUClast \quad (3)$$

Correspondingly, volume of distribution (V_d) was calculated from $(CL_{Total})/k_e$, where CL_{Total} represents the total body clearance.

$$CLTotal = Dose/AUCinf \quad (4)$$

$$Vd = CLTotal/ke \quad (5)$$

2.7. Statistical analysis

Results were expressed as mean ± S.D for n = 3 by using column statistics in Graph Pad, Prism04 Software. Unpaired '*t*' test was used to calculate the statistical significant difference between mean values of two groups. One-way and two-way ANOVA tests were used for comparison between different groups.

3. Results

3.1. Synthesis and confirmation of 5-FU-rHSA and 5-FU-rHSA-PEG

In present investigation, 5-FU-rHSA and 5-FU-rHSA-PEG were designed and synthesized (Scheme 1) for customizing the parenteral nanoformulations to achieve a long circulation half-life. The ^{1}H NMR spectrum of 5-FU-CH_2OOCH_3 displayed the peaks at 2.7768 and 2.7603 ppm, respectively for the protons of $-CH_2$ and $-CH_3$ functional group (Scheme 1 and Fig. 1). On the other hand, ^{1}H NMR spectrum of 5-FU template exhibited the peaks in the range of 7.64-7.65 ppm for CH=CF of 5-FU (Fig. 1). Following this, the synthesis of 5-FU-CH_2COOH (Scheme 1) was confirmed by ^{1}H NMR that depicted the presence of H_2C-COO- at 4.54 ppm (Singlet) (Fig. 1). Next, FT-IR spectroscopy was used to confirm the synthesis of 5-FU-rHSA biomacromolecule (Scheme 1, Fig. 1 and Suppl. Table 1). The spectrum of 5-FU displayed peaks at 1081.90 cm^{-1}, 1239.83 cm^{-1}, and 1348.43 cm^{-1} for fluorine, 1639.20 cm^{-1} for —C=O and 3526.57 cm^{-1} for —NH group. However, in spectrum of 5-FU-rHSA, the peaks of fluorine were slightly shifted, respectively at 1043.25 cm^{-1} and 1251.48 cm^{-1}. In addition, the peaks for —NH—C=O and —COOH were appeared respectively at 1668.46 cm^{-1} and 1251.48 cm^{-1} (Fig. 1 and Suppl. Table 1). Correspondingly, the synthesis of 5-FU-rHSA-PEG was also confirmed by FT-IR spectroscopy (Scheme 1, Fig. 1 and Suppl. Table 1). The spectrum of 5-FU-rHSA-PEG exhibited peaks at 1160.78 cm^{-1} and 1248.05 cm^{-1} for fluorine as well as 1688.29 cm^{-1} for —NH—C=O group. Hence, FT-IR spectra evinced that 5-FU persisted its characteristics in protein matrix and steps of conjugation did not impact the chemical stability of drug. In addition, Bradford assay method [44] and SDS-PAGE were also implicated to determine the conjugation efficiency of drug to protein matrix. The conjugation efficiency of 5-FU to rHSA was estimated to be 67.2%. The molecular weight of 5-FU-rHSA and 5-FU-rHSA-PEG was determined respectively in the range of 66–69 *K*Da and 71–73 *K*Da as compared to 66–67 *K*Da for rHSA alone (Suppl. Fig. 1). Hence, the tailored conjugates (5-FU-rHSA or 5-FU-rHSA-PEG) contain 13–14 mM of 5-FU/mM of rHSA.

3.2. Preparation and characterization of 5-FU-rHSA-NPs and 5-FU-rHSA-PEG-NPs

5-FU-rHSA-PEG-NPs and 5-FU-rHSA-NPs were prepared by using desolvation method [39]. Acetone was used as desolvating agent to precipitate the protein in aqueous phase [45]. The mean

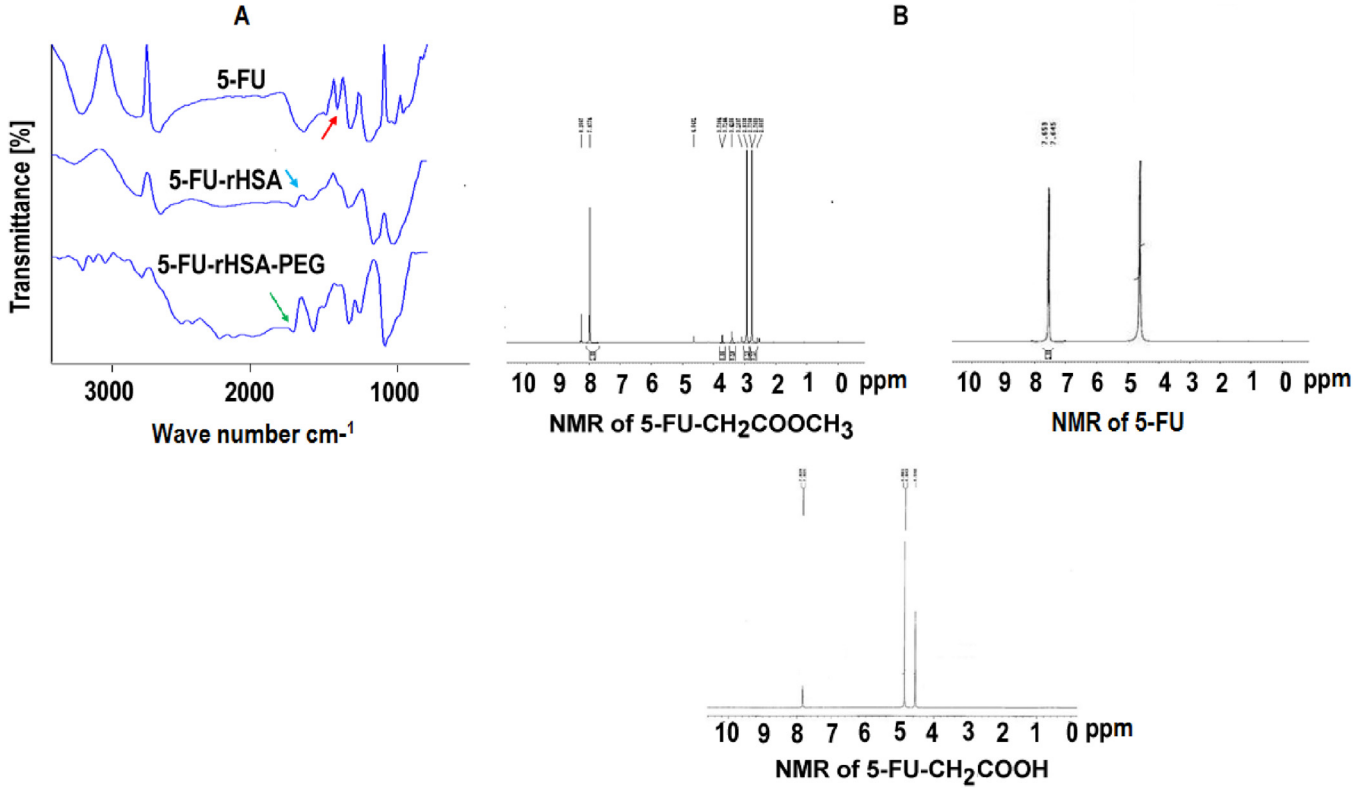

Fig. 1. A) FT-IR spectroscopy of 5-FU, 5-FU-rHSA and 5-FU-rHSA-PEG scanned between 4000 and 400 cm^{-1} at a resolution of 4 cm^{-1}; B) ^{1}H NMR spectrum of 5-FU, 5-FU-CH_2COOCH_3 and 5-FU-CH_2COOH.

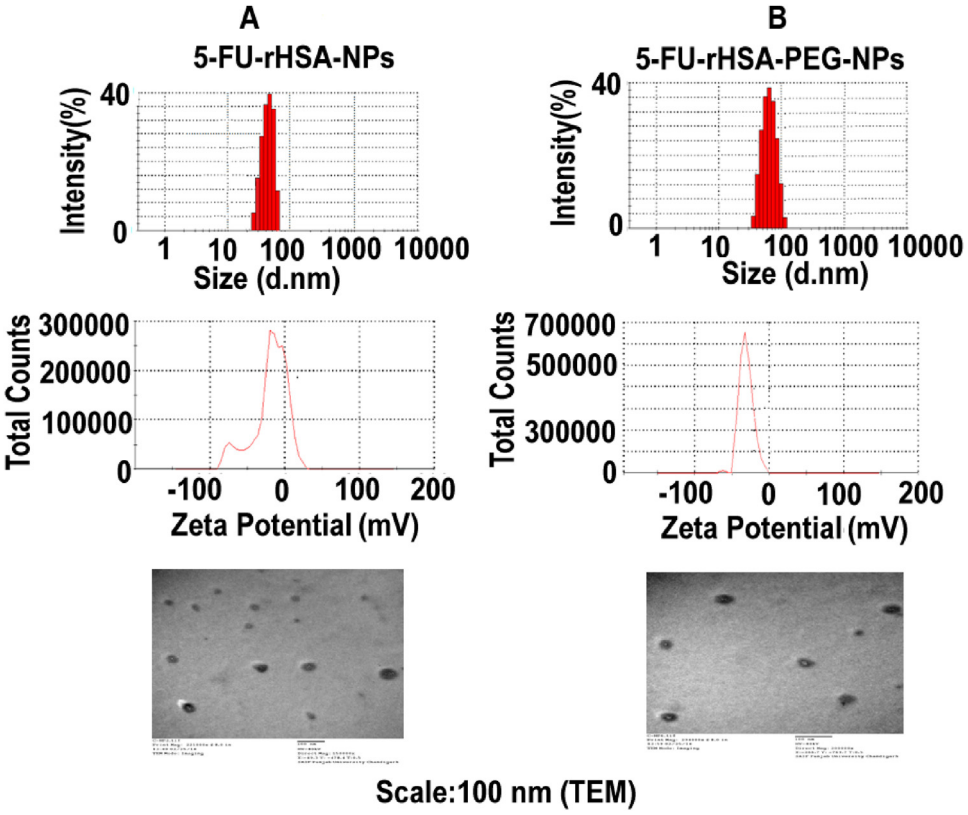

Fig. 2. Particle size distributions, zeta-potential and transmission electron microscopy (TEM) of A) 5-FU-rHSA-NPs and B) 5-FU-rHSA-PEG-NPs. Scale bar ~100 nm in TEM.

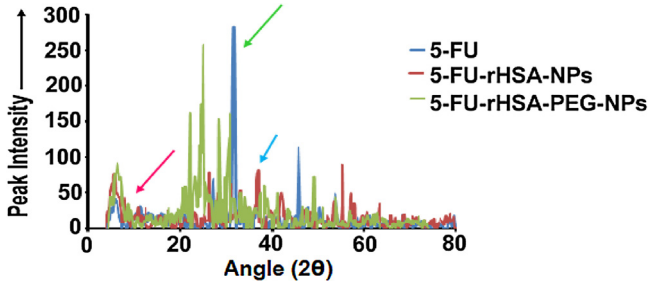

Fig. 3. Powder X-ray diffraction (PXRD) pattern of 5-FU, 5-FU-rHSA-NPs and 5-FU-rHSA-PEG-NPs scanned between 5 and 80° at 2θ.

particle size of 5-FU-rHSA-NPs was measured to be 44.3 ± 5.8 nm, significantly ($P < 0.05$) lesser than 65.7 ± 7.2 nm of 5-FU-rHSA-PEG-NPs (Fig. 2A–B). Correspondingly, zeta-potential of 5-FU-rHSA-NPs was estimated to be −10.2 ± 2.6 mV significantly ($P < 0.05$) smaller than −25.8 ± 3.5 mV of 5-FU-rHSA-PEG-NPs (Fig. 2A–B). TEM photomicrographs taken at the scale of 100 nm substantiated that both 5-FU-rHSA-NPs and 5-FU-rHSA-PEG-NPs were smooth, spherical and regular in shape (Fig. 2A–B). The structural architecture of tailored nanoformulations was elucidated using PXRD technique. The XRD pattern of 5-FU was noticed to be crystalline in nature (blue arrow) (Fig. 3). In contrast, amorphous lattice was discerned for 5-FU-rHSA-NPs owing to the presence of diffused peaks (red arrow). Corresponding to 5-FU-rHSA-NPs, the amorphous nature was also retained in 5-FU-rHSA-PEG-NPs due to the presence of brushes of hydrophilic PEG polymer (green arrow) (Fig. 3). The crystallite size of 5-FU was calculated to be 102.96 nm in comparison to 35.21 nm and 57.62 nm of 5-FU-rHSA-NPs and 5-FU-rHSA-PEG-NPs, respectively. However, the crystallite size may not be correlated with the mean particle size of tailored nanoformulations.

3.3. *In-vitro* drug release analysis

In-vitro drug release study was carried out using dialysis membrane technique [47]. 5-FU solution displayed a maximum release of 99.5% in PBS (pH ~ 7.4) at 0.5 h. On the other hand, 5-FU-rHSA-NPs and 5-FU-rHSA-PEG-NPs only released 10.9% and 9.23%, respectively in PBS (pH ~ 7.4) without any significant difference ($P > 0.05$) (Fig. 4A–B). Continuation to this, addition of 20% v/v serum to PBS (pH ~ 7.4) further boosted the drug release. The tailored nanoformulations, 5-FU-rHSA-NPs and 5-FU-rHSA-PEG-NPs released 78.26% and 48.9% of the 5-FU in 48 h, significantly ($P < 0.05$) higher than the amount of drug released by 5-FU-rHSA-NPs and 5-FU-rHSA-PEG-NPs in PBS (pH ~ 7.4) only (Fig. 4A–B).

3.4. *5-FU-rHSA-PEG-NPs superiorly inhibited cell proliferation in HT-29 cells*

The cytotoxicity of 5-FU solution, 5-FU-rHSA-NPs and 5-FU-rHSA-PEG-NPs was measured in HT-29 cells using standard cell proliferation assay [50]. 5-FU-rHSA-PEG-NPs displayed the IC_{50} of 3.7 μM significantly ($P < 0.05$) lower than 6.8 μM of 5-FU-rHSA-NPs and 11.2 μM of 5-FU solution, respectively (Fig. 5). Correspondingly, there was significance ($P < 0.05$) difference between the IC_{50} of 5-FU-rHSA-NPs and 5-FU, respectively.

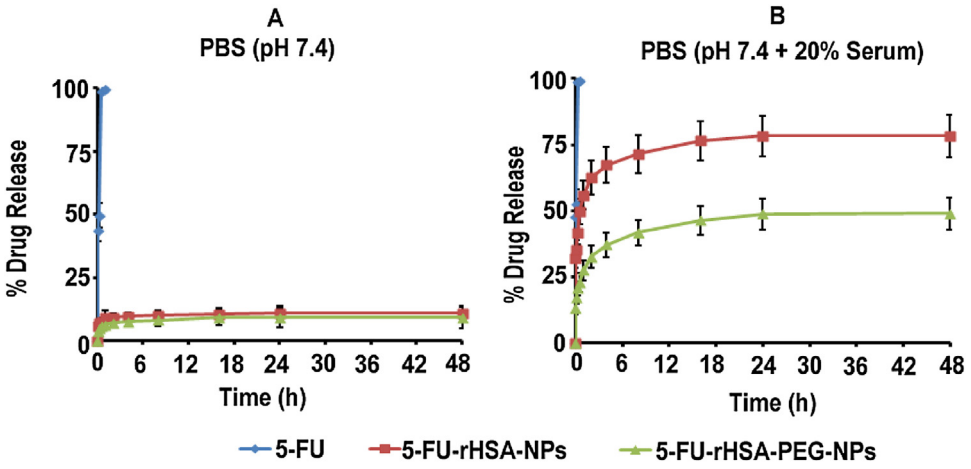

Fig. 4. *In-vitro* drug release of 5-FU solution, 5-FU-rHSA-NPs and 5-FU-rHSA-PEG-NPs carried out in A) phosphate buffer saline (PBS, pH ~ 7.4) and, B) PBS (pH ~ 7.4, with 20% serum) at 37 °C and 100 rpm, as recommended for dissolution testing of parenteral products.

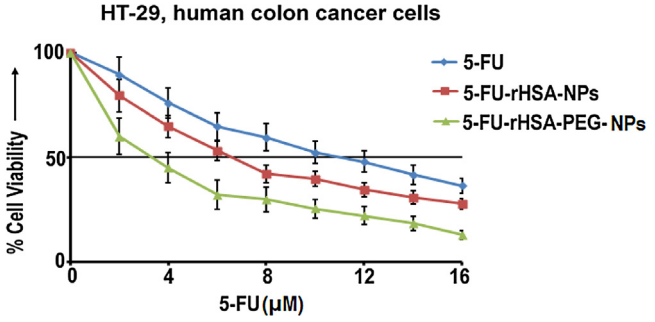

Fig. 5. Percent cell viability analysis of HT-29, human colon cancer cells following treatment with 5-FU, 5-FU-rHSA-NPs and 5-FU-rHSA-PEG-NPs for 72 h using standard cell proliferation assay.

Table 1
One-compartmental pharmacokinetic analysis of 5-FU, 5-FU-rHSA-NPs and 5-FU-rHSA-PEG-NPs administered to male mice through intravenous route of administration at the dose equivalent to 12 mg/kg of 5-FU.

	Nanoformulations		
Parameters	5-FU[a,*]	5-FU-rHSA-NPs[a,*]	5-FU-rHSA-PEG-NPs[a,*]
K_e (h^{-1})	2.303 ± 0.105	0.46 ± 0.08	0.13 ± 0.04
$t_{1/2}$ h^{-1}	0.30 ± 0.09	1.50 ± 0.08	5.33 ± 0.15
AUC_{last} (μg h/ml)	50.57 ± 4.72	323.72 ± 12.49	966.78 ± 18.94
AUC_{inf} (μg h/ml)	70.28 ± 8.95	393 ± 20.32	1582.93 ± 33.25
C_L (Lh^{-1})	0.17 ± 0.04	0.03 ± 0.008	0.007 ± 0.001
V_d (L)	0.073 ± 0.06	0.065 ± 0.052	0.05 ± 0.011
AUMC (μg h^2/ml)	13.51 ± 2.63	644.39 ± 8.72	4155.081 ± 25.68
MRT (h^{-1})	0.26 ± 0.05	1.63 ± 0.42	2.62 ± 0.21

Note: 5-FU: 5-Fluorouracil, 5-FU-rHSA-NPs: 5-Fluoruracil conjugated recombinant human serum albumin nanoparticles, 5-FU-rHSA-PEG-NPs: 5-Fluorouracil conjugated poly (ethylene glycol) anchored recombinant human serum albumin nanoparticles.

[a] Each experiment was carried out in triplicate (n = 3).

[*] P < 0.001 (One-way ANOVA test).

3.5. 5-FU-rHSA-PEG-NPs exhibited longer circulation half-life in preclinical analysis

The pharmacokinetic elements of tailored nanoformulations were analyzed *in vivo*. The pharmacokinetic parameters and plasma concentration-time profile curves were calculated, compiled and analyzed using one-compartmental parameters (Table 1 and Fig. 6). 5-FU-rHSA-PEG-NPs documented 0.13 ± 0.04 h^{-1} of elimination rate constant (k_e) significantly (P < 0.001) lower than 0.46 ± 0.08 h^{-1} and 2.303 ± 0.105 h^{-1} of 5-FU-rHSA-NPs and 5-FU solution, respectively. Consistently, 5-FU-rHSA-PEG-NPs reported the half-life ($t_{1/2}$) of 5.33 ± 0.15 h significantly (P < 0.001) higher than 1.50 ± 0.08 h and 0.30 ± 0.09 h of 5-FU-rHSA-NPs and 5-FU solution, respectively. Furthermore, 5-FU-rHSA-PEG-NPs displayed the AUC_{last} of about 966.78 ± 18.94 μg.h/ml, significantly (P < 0.001) higher than 323.72 ± 12.49 μg·h/ml and 50.57 ± 4.72 μg·h/ml of 5-FU-rHSA-NPs and 5-FU solution, respectively (Table 1). Hence, *in-vivo* analysis substantiated the prolonged release pattern and enhanced drug exposure of 5-FU from tailored nanoformulations upon administration through *i.v* route. Correspondingly, 5-FU-rHSA-PEG-NPs also demonstrated the superiority over 5-FU-rHSA-NPs and 5-FU solution in terms of mean residence time (MRT), volume of distribution (V_d) and total body clearance (CL_{Total}) (Table 1).

4. Discussion

Nanomedicines may become the game changers if these are systematically designed, optimized and characterized with critical parameters. In present investigation, 5-FU was primarily conjugated to rHSA (5-FU-rHSA) and later tailored biomacromolecule was tethered with PEG (5-FU-rHSA-PEG) by covalent-coupling method [43] for shaping the stealth character (Scheme 1, Fig. 1 and Suppl. Table 1). Large molecular weight (20–50 kDa) PEG has been proven useful for extending the blood circulation time, although it enhances the size of nanoparticles. However, large size nanoparticles are complicated to clear from the kidney and preferably, deposited by the liver. Hence, to avoid liver clearance, attachment of low molecular weight PEG (2000–5000 Da) has been advocated to extend the *in vivo* half-life of nanoparticles. In addition, chain length, shape, and density of PEG also influence the extent of hydrophilicity and phagocytosis [52]. The density of PEG in the range of 0.5-5% w/w was optimized to be able to remarkably reduce the amount of protein as compared to unmodified nanoparticles [53]. Hence, it is apparent that 5-FU-rHSA-PEG holds compelling evidences to be used for customizing the nanoparticles (Fig. 2A–B). Further, 5-FU-rHSA-NPs and 5-FU-rHSA-PEG-NPs were prepared by desolvation technique using acetone as desolvating agent [39,45]. Using molecular dynamics techniques, we reported that acetone is a favourable desolvating agent in comparison to ethanol, as it generates smaller size nanoparticles of protein (< 100 nm) with uniform size distribution (Fig. 2A–B) [45]. Surface charge is a vital physicochemical element that influences the stability and fate of nanoparticles in physiological *milieu*. Usually, the surface charge of ≥ ± 25 mV is desirable for achieving a sta-

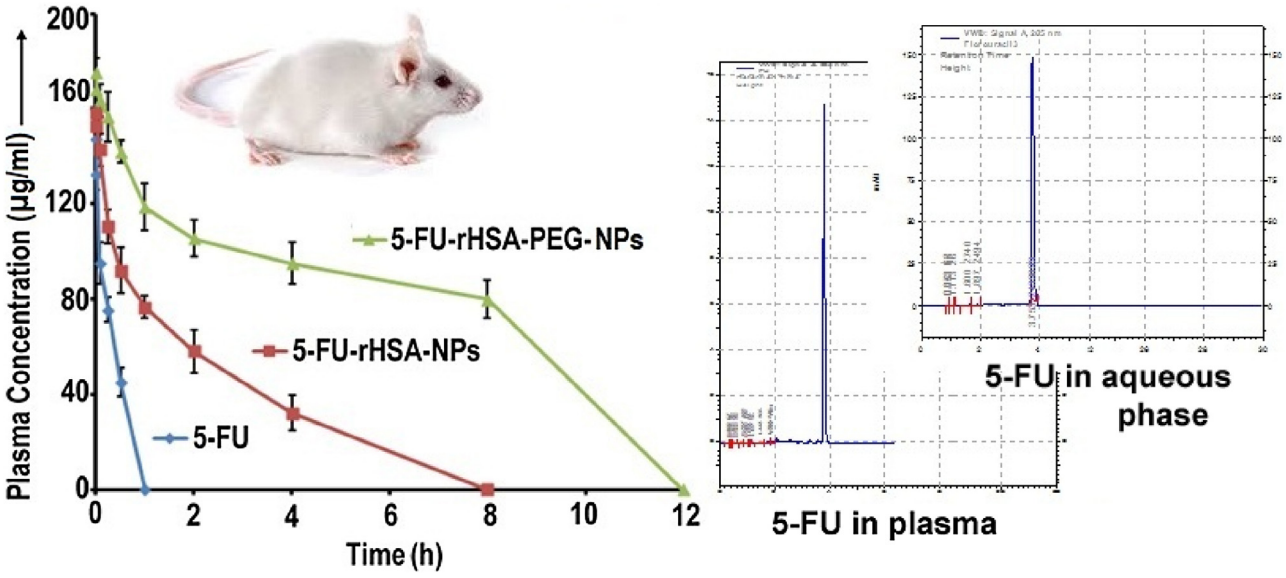

Fig. 6. Plasma-concentration (µg/ml) vis-à-vis time profile (h) curve of 5-FU solution, 5-FU-rHSA-NPs and 5-FU-rHSA-PEG-NPs administered through *i.v* route in Swiss albino male mice at the dose of 12 mg/kg of 5-FU along with representative chromatograms.

ble dispersion. High positive or negative surface charge generates larger repulsive forces, whereas repulsion between nanoparticles with identical electric charge prevents aggregation and thus ensures easy redispersion [54,55]. Moreover, surface charge also determines various physiological activities of nanoparticles like circulation time, metabolism, clearance, and immune response [55,56]. Therefore, owing to the presence of negative surface charge (Fig. 2A–B), a highly stable and efficacious nanosuspension of 5-FU-rHSA-NPs and 5-FU-rHSA-PEG-NPs may be expected in both *in vitro* and *in vivo* testing conditions. Binding of plasma proteins is an opening mechanism for RES to recognize the injected nanoparticles that consequently causes a huge loss of the administered dose. Macrophages in liver (Kupffer cells) recognize the opsonized nanoparticles via scavenger receptors. Liver, spleen and bone marrow are the major RES organs responsible for the fate of nanoparticles. All macrophages reported a net negative surface charge. On the other hand, activated macrophages bear a lower zeta-potential and a higher isoelectrophoretic point than resident and elicited macrophages. This may be attributed to higher density of sialic acid residues on the surface of activated macrophages [56,57]. Hence, owing to electrophoretic repulsion between negatively charged 5-FU-rHSA-PEG-NPs and negatively charged macrophages, a delay in the fate of nanoparticles and prolonged plasma half-life may be anticipated.

Nanoparticles shape directly persuades the cellular uptake [58]. The cellular uptake of nanoparticles >100 nm has followed the order of nanorods > nanospheres > nanocylinders and nanocubes [58–60]. Interestingly, nanospheres were endocytosed more rapidly than nanorods when nanoparticles size was <100 nm [59,60]. Therefore, owing to spherical shape of 5-FU-rHSA-NPs and 5-FU-rHSA-PEG-NPs (Fig. 2A–B), a higher cellular uptake may be anticipated in cancer cells. Furthermore, PXRD confirmed the amorphous lattice of 5-FU-rHSA-NPs and 5-FU-rHSA-PEG-NPs (Fig. 3). Generally, due to asymmetrical structural lattice, the amorphous phase demands minimal energy and consequently offers higher solubility and bioavailability of drugs [36]. Hence, sub-cellular particle size, negative surface charge, spherical shape and amorphous lattice attributes of 5-FU-rHSA-NPs and 5-FU-rHSA-PEG-NPs, were found to be decisive for delivering through *i.v* route of administration for offering prolonged release and improved circulation half-life.

Following this, *in vitro* release study of 5-FU from 5-FU-rHSA-NPs and 5-FU-rHSA-PEG-NPs was performed in PBS (pH ~ 7.4) in presence and absence of serum (Fig. 4A–B). Conjugation of 5-FU with stealth protein biomacromolecule prevented the superfluous release of drug in PBS (pH ~ 7.4) as compared to free 5-FU. Hence, 5-FU would not produce toxicity to normal tissues owing to erratic biodistribution. However, addition of serum to PBS (pH ~ 7.4) promoted the prolonged release of 5-FU from 5-FU-rHSA-NPs. Human serum contains proteolytic enzyme, chymase. It is well know that albumin is a substrate for chymase. Chymase hydrolyzes the albumin uniquely and the resulting fragments retained disulfide-linkage likely between Cys-75 and Cys-90 [61]. Thus, gradual degradation of rHSA in 5-FU-rHSA-NPs offered constant release of 5-FU for prolonged period of time. However, owing to the presence of higher negative surface charge on 5-FU-rHSA-PEG-NPs, the rate of degradation was slower in comparison to 5-FU-rHSA-NPs that subsequently suppressed the release of 5-FU. Therefore, we may correlate and predict the longer *in vivo* circulation half-life of 5-FU-rHSA-PEG-NPs (Fig. 4A–B).

The therapeutic potential of 5-FU solution, 5-FU-rHSA-NPs and 5-FU-rHSA-PEG-NPs was investigated in HT-29 cells and expressed in terms of IC_{50} value (Fig. 5). The IC_{50} of 5-FU-rHSA-PEG-NPs was estimated to be ~3.02 and ~1.83 folds lower than the 5-FU solution and 5-FU-rHSA-NPs, respectively. Hypoxia-inducible factor (HIF-1α) protein is over-expressed in many human cancers and is a major cause of resistance to drugs. HIF-1α up-regulation decreases the effectiveness of several anticancer agents including 5-FU in HT-29 cells, because it induces the expression of drug efflux transporters (P-gp), alters DNA repair mechanisms and modifies the balance between pro- and antiapoptotic proteins [62]. Previous reports indicated that PEG inhibits the ATPase enzyme that is involved in the functioning of P-gp efflux pump proteins, thus modulates the transport of therapeutic moiety [63,64]. Hence, we propose that the lower IC_{50} and enhanced cytotoxicity of 5-FU-rHSA-PEG-NPs may be attributed to greater endocytosis of nanoparticles by HT-29 cells in comparison to 5-FU solution and 5-FU-rHSA-NPs, respectively.

In last, pharmacokinetic parameters of 5-FU, 5-FU-rHSA-NPs and 5-FU-rHSA-PEG-NPs were assessed and compared (Table 1 and Fig. 6). 5-FU-rHSA-PEG-NPs displayed the superior pharmacokinetic profile in comparison to 5-FU-rHSA-NPs and 5-FU solution,

respectively. We monitored ~17.76 folds increment in the circulation half-life of 5-FU when injected as 5-FU-rHSA-PEG-NPs as compared to 5-FU solution. Correspondingly, other pharmacokinetic parameters like AUC_{last} and MRT were also improved upon administration of 5-FU-rHSA-PEG-NPs (Table 1). AUC_{last} is an imperative parameter to measure the drug exposure. Notable in these results was approximately ~2.98 folds increase in the AUC_{last} by 5-FU-rHSA-PEG-NPs over the 5-FU-rHSA-NPs and ~19.11 folds hike over the 5-FU solution in scheduled dose-dosage regimen. Moreover, 5-FU-rHSA-PEG-NPs displayed higher MRT in plasma that confirmed the stealth character and permitted the nanoformulation to circulate for longer period of time by avoiding RES uptake.

5. Conclusion

5-FU-rHSA-PEG-NPs and 5-FU-rHSA-NPs were successfully customized to offer prolonged release through *i.v* route of administration. *In vitro* and *in vivo* testing parameters indicated that 5-FU-rHSA-PEG-NPs and 5-FU-rHSA-NPs release the drug in sustained fashion in physiological mediums. The therapeutic efficacy and pharmacokinetics of 5-FU-rHSA-PEG-NPs were estimated to be superior than 5-FU-rHSA-NPs under a set of biological techniques. Therefore, 5-FU-rHSA-PEG-NPs formulation may be a potential candidate for testing under a set of stringent parameters for translating in to a clinical product.

Appendix A. Supplementary data

Supplementary data associated with this article can be found, in the online version, at http://dx.doi.org/10.1016/j.colsurfb.2017.04.020.

References

[1] J. Prados, C. Melguizo, R. Ortiz, G. Perazzoli, L. Cabeza, P.J. Alvarez, F. Rodriguez-Serrano, A. Aranega, Anticancer Agents Med. Chem. 13 (2013) 1204.
[2] O. Glehen, F. Kwiatkowski, P.H. Sugarbaker, D. Elias, E.A. Levine, M. De Simone, R. Barone, Y. Yonemura, F. Cavaliere, F. Quenet, M. Gutman, A.A.K. Tentes, G. Lorimier, J.L. Bernard, J.M. Bereder, J. Porcheron, A. Gomez-Portilla, P. Shen, M. Deraco, P. Rat, J. Clin. Oncol. 22 (2004) 3284.
[3] M.H. Cohen, J. Gootenberg, P. Keegan, R. Pazdur, Oncologist 12 (2007) 356.
[4] T. Ogiso, N. Noda, N. Asai, Y. Kato, Jpn. J. Pharmacol. 26 (1976) 445.
[5] H. Masuda, T. Ogiso, N. Noda, Y. Kato, Jpn. J. Pharmacol. 28 (1978) 175.
[6] W.B. Parker, Y.C. Cheng, Pharmacol. Ther. 48 (1990) 381.
[7] D.B. Longley, D.P. Harkin, P.G. Johnston, Nat. Rev. Cancer 3 (2003) 330.
[8] B. Daniel, D. Longley, D. Paul Harkin, P.G. Johnston, Nat. Rev. Cancer 3 (2003) 330.
[9] M. Aprahamian, C. Michel, W. Humbert, J.P. Devissaguet, C. Damge, Biol. Cell 61 (1987) 69.
[10] R.B. Diasio, Z. Lu, J. Clin Oncol. 12 (1994) 2239.
[11] R.L. Schilsky, J. Hohneker, M.J. Ratain, L. Janisch, L. Smetzer, V.S. Lucas, S.P. Khor, R. Diasio, D.D. Von Hoff, H.A. Burris, J. Clin. Oncol. 16 (1998) 1450.
[12] G. Pasut, D. Paolino, C. Celia, A. Mero, A.S. Joseph, J. Wolfram, D. Cosco, O. Schiavon, H. Shen, M. Fresta, J. Control. Release 199 (2015) 106.
[13] W. Cheng, R.G. Compton, Angew Chem. Int. Ed. Engl. 53 (2014) 13928.
[14] Q.Y. Bao, N. Zhang, D.D. Geng, J.W. Xue, M. Merritt, C. Zhang, Y. Ding, Int. J. Pharm. 477 (2014) 408.
[15] A. Lamprecht, H. Yamamoto, T. Hirofumi, Y. Kawashima, J. Control. Release 90 (2003) 313.
[16] N. Ashwanikumar, N.A. Kumar, S.A. Nair, G.S. Kumar, Acta Biomater. 10 (2014) 4685.
[17] S.S. Agasti, A. Chompoosor, C.C. You, P. Ghosh, C.K. Kim, V.M. Rotello, J. Am. Chem. Soc. 131 (2009) 5728.
[18] S.M. Lee, Y.S. Bala, W.K. Lee, N.J. Jo, I. Chung, J. Biomed. Mater. Res. A 101 (2013) 2306.
[19] M.S. Matlapudi, A. Moin, R. Medishetti, K. Rajendra, A.M. Raichur, B.R. Kumar, Curr. Drug Deliv. 12 (2015) 782.
[20] T. Peters, All About Albumin: Biochemistry, Genetics and Medical Applications, Academic Press Limited, San Diego, CA, 1996.
[21] S. Sebak, M. Mirzaei, M. Malhotra, A. Kulamarva, S. Prakash, Int. J. Nanomed. 5 (2010) 525.
[22] K. Kobayashi, Biologicals 34 (2006) 55.
[23] W. Ohtani, Y. Nawa, K. Takeshima, H. Kamuro, K. Kobayashi, T. Ohmura, Anal. Biochem. 256 (1998) 56.
[24] C.J. Hunt, Transfus. Med. Hemother. 38 (2011) 107.
[25] K. Taguchi, K. Yamasaki, H. Seo, M. Otagiri, Pharmaceutics 7 (2015) 255.
[26] O. Akbal, E. Erdal, T. Vural, D. Kavaz, E.B. Denkbas, Artif. Cells Nanomed. Biotechnol. 17 (2016) 1.
[27] Q.L. Thao, H.J. Byeon, C. Lee, S. Lee, E.S. Lee, Y.W. Choi, H.G. Choi, E.S. Park, K.C. Lee, Y.S. Youn, Pharm. Res. 33 (2016) 615.
[28] E.J. Truter, A.S. Santos, W.J. Els, Cell Biol. Int. 25 (2001) 51.
[29] H. Maeda, J. Wu, T. Sawa, Y. Matsumura, K. Hori, J. Control. Release 65 (2000) 271.
[30] H. Maeda, Biconjugate Chem. 21 (2010) 797.
[31] G. Stehle, H. Sinn, A. Wunder, H.H. Schrenk, J.C. Stewart, G. Hartung, W. Maier-Borst, D.L. Heene, Crit. Rev. Oncol. 26 (1997) 77.
[32] A.M. Merlot, D.S. Kalinowski, D.R. Richardson, Front. Physiol. 5 (2014) 299.
[33] J.M. Harris, R.B. Chess, Nat. Rev. Drug Discov. 2 (2003) 214.
[34] T. Sawa, J. Wu, T. Akaike, H. Maeda, Cancer Res. 60 (2000) 666.
[35] G. Pasut, F.M. Veronese, Prog. Polym. Sci. 32 (2007) 933.
[36] J. Madan, R.S. Pandey, U.K. Jain, O.P. Katare, R. Aneja, A. Katyal, Colloids Surf. B: Biointerfaces 107 (2013) 235.
[37] J. Madan, R.S. Pandey, V. Jain, O.P. Katare, R. Chandra, A. Katyal, Nanomedicine 9 (2013) 492.
[38] J. Madan, N. Dhiman, S. Sardana, R. Aneja, R. Chandra, A. Katyal, Anticancer Drugs 22 (2011) 543.
[39] K. Langer, S. Balthasar, V. Vogel, N. Dinauer, H. von Briesen, D. Schubert, D. Int, J. Pharm. 257 (2003) 169.
[40] Y. Niv, B. Schwartz, Y. Amsalem, S.A. Lamprecht, Anticancer Res. 15 (1995) 2023.
[41] K.K. Devadoss, R.P. Subramaniam, Tetrahedron Lett. 53 (2012) 3230.
[42] M. Li, Z. Liang, X. Sun, T. Gong, Z. Zhang, PLoS One 9 (2014) e112888.
[43] K. Kaur, R.K. Sodhi, A. Katyal, R. Aneja, U.K. Jain, O.P. Katare, J. Madan, Colloids Surf. B: Biointerfaces 132 (2015) 225.
[44] M.M. Bradford, Anal. Biochem. 72 (1976) 248.
[45] J. Madan, S.R. Gundala, Y. Kasetti, P.V. Bharatam, R. Aneja, A. Katyal, U.K. Jain, Anticancer Drugs 25 (2014) 704.
[46] H.P. Klung, L.E. Alexander, X-Ray diffraction procedures for polycrystalline and amorphous materials, 2nd ed., John Wiley and Sons, New York, 1954.
[47] P.K. Gupta, C.T. Hung, D.G. Perrier, J. Pharm. Sci. 76 (1987) 141.
[48] R. Puri, R.K. Bhatia, R.S. Pandey, U.K. Jain, O.P. Katare, J. Madan, Drug Dev. Ind. Pharm. 42 (2016) 2020.
[49] I.A. Alvi, J. Madan, D. Kaushik, S. Sardana, R.S. Pandey, A. Ali, Anticancer Drugs 22 (2011) 774.
[50] T. Mosmann, J. Immunol. Methods 65 (1983) 55.
[51] A.C. de Mattos, N.M. Khalil, R.M. Mainardes, Braz. J. Pharm. Sci. 49 (2013) 117.
[52] J.J.F. Verhoef, T.J. Anchordoquy, Drug Deliv. Transl. Res. 3 (2013) 499.
[53] R. Gref, M. Luck, P. Quellec, M. Marchand, E. Dellacherie, S. Harnisch, T. Blunk, R.H. Muller, Colloids Surf. B: Biointerfaces 18 (2000) 301.
[54] S. Patila, A. Sandberg, E. Heckert, W. Self, S. Sea, Biomaterials 28 (2007) 4600.
[55] N. Seetapan, P. Bejrapha, W. Srinuanchai, U.R. Ruktanonchai, Micron 41 (2010) 51.
[56] Y. Qiu, Y. Liu, L.M. Wang, L.G. Xu, R. Bai, Biomaterials 31 (2010) 7606.
[57] A. Varki, P. Gagneux, Ann. N. Y. Acad Sci. 1253 (2012) 16.
[58] B. Damascelli, G. Cantu, F. Mattavelli, P. Tamplenizza, P. Bidoli, E. Leo, F. Dosio, A.M. Cerrotta, G. Di Tolla, L.F. Frigerio, F. Garbagnati, R. Lanocita, A. Marchiano, G. Patelli, C. Spreafico, V. Ticha, V. Vespro, F. Zunino, Cancer 92 (2001) 2592.
[59] X. Zhu, B.D. Silva, X. Zou, B. Shen, Y. Sun, W. Feng, F. Li, RSC Adv. 4 (2014) 23580.
[60] S. Joshi, J.A. Ellis, C.W. Emala, J. Neuroanaesthesiol Crit. Care 1 (2014) 108.
[61] W.W. Raymond, S.W. Ruggles, C.S. Craik, G.H. Caughey, J. Biol. Chem. 278 (2003) 34517.
[62] J. Chen, Z. Ding, Y. Peng, F. Pan, J. Li, L. Zou, Y. Zhang, H. Liang, PLoS One 9 (2014) e98882.
[63] M. Werle, J. Pharm. Sci. 97 (2008) 60.
[64] M. Werle, Pharm. Res. 25 (2008) 500.